Organic photovoltaic bulk heterojunctions with spatially varying composition.

Paul M. Haney[1]
[1] *Center for Nanoscale Science and Technology, National Institute of Standards and Technology, Gaithersburg, Maryland 20899-6202, USA*

Models of organic bulk heterojunction photovoltaics which include the effect of spatially varying composition of donor/acceptor materials are developed and analyzed. Analytic expressions for the current-voltage relation in simplified cases show that the effect of varying blend composition on charge transport is minimal. Numerical results for various blend compositions, including the experimentally relevant composition of a donor-rich region near the cathode (a "skin layer" of donor material), show that the primary effect of this variation on device performance derives from its effect on photocharge generation. The general relation between the geometry of the blend and its effect on performance is given explicitly. The analysis shows that the effect of a skin layer on device performance is small.

I. INTRODUCTION

Photovoltaic devices consisting of two types of organic materials (referred to as donor (D) and acceptor (A)) have attracted considerable scientific interest in recent years. Their operation consists of the generation of an exciton in the donor molecule, which is then disassociated into free carriers at the D-A interface (the electron is transferred to the acceptor molecule's lowest unoccupied molecular orbital (LUMO), leaving a hole in the donor molecule's highest occupied molecular orbital (HOMO)). Carriers which avoid recombination are then collected by contacts. The geometry first studied consisted of single D and A layers, with a single planar interface [1]. The resulting efficiencies were low (1 %), owing in part to the short exciton diffusion length (10 nm) - only excitons within this short distance from the interface lead to free carriers. It was subsequently discovered that blending D and A together throughout the device thickness led to increased efficiencies [2], now above 5 % [3–5]. This increase in efficiency is attributed to an increase in D-A interfacial area; carrier transport is sufficiently robust to the disorder present in the blend to accommodate reasonable quantum efficiencies. If the organic blend is completely homogeneous, the contacts on the device must be different in order to break spatial symmetry and permit a nonzero short-circuit current in a preferred direction. The key difference between the contacts is their work function: a lower (higher) work function ensures that the contact preferentially collects and injects electrons (holes). Hence it is understood that the cathode collects electrons, and the anode collects holes.

A major thrust of experimental efforts has been to attain control over blend morphology in order to optimize both exciton disassociation and charge transport. Recent examples include using nanoimprint lithography to control the structure of the donor-acceptor molecules' interfacial profile [6], or using a graded donor-acceptor blend to optimize both carrier collection and transport [7]. A key challenge of engineering blend morphology is the measurement and characterization of the structure of the organic blend. Techniques for accomplishing this include atomic force microscopy [8], ellipsometry [9], and X-ray photoelectron spectroscopy [10]. These techniques have revealed that typical methods for fabricating devices lead to a layer of enhanced donor molecule density at the cathode, which has been attributed to surface energy differences between the active layer and other components [10]. This would seem to present an impediment to good device performance: the cathode collects electrons, but in its vicinity is mostly holes! Nevertheless, internal quantum efficiencies of 90 % have been observed in these materials [11], indicating that charge collection is still a relatively efficient process [9].

In this work, I theoretically study the effect of a nonuniform blend on organic photovoltaic (OPV) device performance. I employ a drift-diffusion equation to describe electron and hole transport, a field and temperature dependent generation and recombination rate that captures the exciton physics, and the Poisson equation for electrostatics. To this model I add the effect of a spatially varying effective density of states (EDOS) (note that "density of states" refers to the number of states per volume per unit energy, whereas "effective density of states" refers to the number of states per volume). Part I describes details of the model. In part II, I present analytic solutions for the transport under certain approximations; these point to the fact that the effect of a spatially varying EDOS on charge transport is small. In part III, I present numerical results which indicate that the primary effect of a spatially varying EDOS is on the charge generation and ensuing $J_{\rm sc}$. It is shown that this can be understood in terms of the overall geometry of the composition profile. I conclude that since the skin layer near the cathode is geometrically small on the scale of the device thickness, its effect on performance is similarly small.

II. MODEL

The model used to describe the system is similar to that found in Ref. 14. Its basic equations are presented here in dimensionless form. Table I shows the variable

scalings used. The dimensionless drift-diffusion/Poisson equations including a spatially varying EDOS are given as [12]:

$$\begin{aligned} J_n &= n\left(-\frac{\partial}{\partial x}V - \frac{\partial}{\partial x}\left[\ln N\right]\right) + \frac{\partial}{\partial x}n \ , \\ J_p &= f_\mu\left[p\left(-\frac{\partial}{\partial x}V + \frac{\partial}{\partial x}\left[\ln P\right]\right) - \frac{\partial}{\partial x}p\right] \ , \\ -\frac{\partial}{\partial x}J_n &= \frac{1}{f_\mu}\frac{\partial}{\partial x}J_p = G - R \ , \qquad (1) \\ \frac{\partial^2}{\partial x^2}V &= p - n \ , \qquad (2) \end{aligned}$$

where $f_\mu = \mu_h/\mu_e$ is the ratio of hole to electron mobility, G is the carrier density generation rate, and R is the recombination. $N(x)$ and $P(x)$ are the spatially-dependent electron and hole effective density of states, respectively. n and N are related via: $n = Ne^{-(E_c - E_{F,n})/kT}$, where $E_{F,n}$ is the electron quasi-Fermi level, E_c is the conduction band edge, and all quantities are position-dependent (the densities are assumed to be such that the system is in a nondegenerate regime). p and P are related similarly. $N(x)$ and $P(x)$ are fixed material parameters, while n and p are system variables that depend on applied voltage and illumination. For a single band semiconductor, the effective density of states N is given by $\frac{1}{\sqrt{2}}\left(\frac{m_n^* k_{\rm B} T}{\pi\hbar^2}\right)^{3/2}$, where m_n^* is the effective electron mass. In the present context of organic materials, N is more properly understood as the number of HOMO states per unit volume, and is proportional to the donor molecule density.

TABLE I: Normalization to dimensionless variables. In the below N_0 is the characteristic density (typically chosen to be on the order of 10^{-25} m^{-3}) D_n is the electron diffusivity, ϵ is the dielectric constant of the organic blend, q is the magnitude of the electron charge, T is the temperature, and $k_{\rm B}$ is Boltzmann's constant.

Quantity	Normalization
density	N_0
position	$\sqrt{\epsilon k_B T/(q^2 N_0)} \equiv x_0$
charge current	$qD_n N_0/x_0$
electric potential	$k_{\rm B}T/q$
rate density	$x_0^2/N_0 D_n$

The boundary conditions are given as:

$$\begin{aligned} n(0) &= N(0)\, e^{-E_g + \phi_L}, \\ p(0) &= P(0)\, e^{-\phi_L}, \\ n(L) &= N(L)\, e^{-\phi_R}, \\ p(L) &= P(L)\, e^{-E_g + \phi_R}, \qquad (3) \end{aligned}$$

where L is the device thickness (this represents placing the anode at $x = 0$, and the cathode at $x = L$). $\phi_{L(R)}$ is the absolute value of the difference between HOMO (LUMO) and left (right) contact Fermi level. The boundary condition for the Poisson equation is:

$$V(L) - V(0) = (E_g - \phi_L - \phi_R) - V_{\rm A}, \qquad (4)$$

where $V_{\rm A}$ is the applied voltage (with the sign convention above, $V_{\rm A} > 0$ corresponds to forward bias).

I consider only bimolecular recombination, with (dimensionless) form:

$$R = \left(np - n_i^2\right) \ , \qquad (5)$$

where $n_i^2 = n_0 p_0$, and n_0 (p_0) is the equilibrium electron (hole) density. The carrier generation rate density is taken to be spatially uniform. As described in Ref. [14], adding the exciton density as a system variable modifies the source term in Eq. (1):

$$(G - R) \rightarrow \tilde{P} \times G_0 - \left(1 - \tilde{P}\right) \times R, \qquad (6)$$

where G_0 is the exciton density generation rate, and $\tilde{P}$ is a field and temperature dependent factor which represents the probability for an exciton to disassociate into free electron and hole [14, 20]. The field and temperature dependence is described by Braun's extension of Onsager's theory of ion disassociation in electrolytes [21].

Charge recombination and generation also generally depend on the donor and acceptor effective density of states. The total source term of Eq. (1) (denoted here by $U(x)$) is therefore of the generic form:

$$\begin{aligned} U(x) &= \tilde{P} \times G_0 \times g\left[N(x), P(x)\right] - \\ &\quad \left(1 - \tilde{P}\right) \times R \times r\left[N(x), P(x)\right]. \qquad (7) \end{aligned}$$

The appropriate forms for g and r depend on several factors, such as the dependence of the optical absorption and D-A interface area on relative D-A composition.

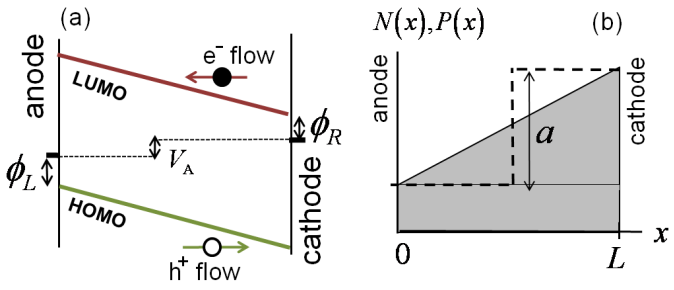

FIG. 1: (a) Energy diagram for device model; cartoon of particle flow depicts dark current in forward bias. (b) Spatial dependence of EDOS: linear variation (shaded region), and step-like change (dotted line) in both $N(x)$ and $P(x)$.

III. ANALYTIC CASES

The set of equations described in Eq. (1) can be solved analytically for limiting cases, which can provide some insight into the effect of a spatially varying EDOS on the transport. Two cases are considered here: the first is an exponentially varying EDOS (which can be extrapolated to a linearly varying EDOS), and the second is an abrupt, step-like change in the EDOS. I present both solutions first and discuss the physics they describe second.

In both cases the electric field E is taken to be spatially uniform (so that $V(x) = -Ex$), and recombination is ignored. I suppose further that G is constant, and independent of N, P (that is, $g(N, P) = 1$ in Eq. (7)). The exponentially varying EDOS is parameterized as:

$$N(x) \;=\; P(x) = A_0\, e^{ax/L}, \tag{8}$$

where $A_0 = a/\left(e^a - 1\right)$ ensures that the total number of states is independent of a. Substituting the expressions for electron (hole) current density $J_{n(p)}$ into the equation of continuity (Eq. (1)) results in a second order differential equation for the electron (hole) density n (p). For the EDOS of Eq. (8), the resulting general solution is:

$$\begin{aligned} n(x) &= c_1 e^{(a-f)x} + c_2 + \frac{Gx}{a-f}\ , \\ p(x) &= c_1 e^{(a+f)x} + c_2 + \frac{Gx}{a+f}, \end{aligned} \tag{9}$$

where $c_1,\ c_2$ are determined by the boundary conditions of Eq. (3). From this solution the current density can be obtained directly.

I express the resulting current-voltage relation as a sum of dark current and light current:

$$J(V_{\rm A}) = J_D + G J_L\ , \tag{10}$$

Both light and dark currents are well described by expanding to lowest order in the spatial variation of EDOS parameter a; I take $\phi_L = \phi_R = 0$, and express the applied voltage dependence in terms of $f = \left(E_g - qV_{\rm A}\right)/k_{\rm B}T$. f is bigger than 1 in the region of interest [15], leading to the further approximation that $\sinh f \approx \cosh f \approx 1/2\, e^f$. It's useful to express current-voltage relation in terms of that for a uniform EDOS and electric field:

$$\begin{aligned} J_D^0 &= \frac{2f\left(e^{V_{\rm A}} - 1\right)}{L\left(e^f - 1\right)e^{V_{\rm A}}} \\ J_L^0 &= L\left(\frac{2}{f} - \coth\left(\frac{f}{2}\right)\right). \end{aligned} \tag{11}$$

The dark and light current for the exponentially varying profile of Eq. (8) is then found to be:

$$\begin{aligned} J_D^{\rm exp} &\approx J_D^0\left(1 + a^2\left(\frac{1}{12} - \frac{1}{2f}\right) + O\left(a^4\right) + ...\right)\ , \\ J_L^{\rm exp} &\approx J_L^0\left(1 + a^2\left(-\frac{2}{f^3} + e^{-f}\right) + O\left(a^4\right) + ...\right) \end{aligned} \tag{12}$$

I next consider a step function form of $N(x), P(x)$. I use the following form:

$$N(x) = P(x) = \begin{cases} 1 - a/2 & \text{if } x < L/2, \\ 1 + a/2 & \text{if } x \geq L/2. \end{cases} \tag{13}$$

The general solutions for each region ($x < L/2,\ x > L/2$) are of the form given by Eq. (9) with a=0. In addition to the boundary condition Eq. (3), there's an additional boundary condition for this EDOS of continuity of charge and current density at $x = L/2$. Making the same approximations as above leads to the following dark and light current:

$$\begin{aligned} J_D^{\rm step} &\approx J_D^0\left(1 - a^2 e^{-f/2} + O\left(a^4\right) + ...\right)\ , \\ J_L^{\rm step} &\approx J_L^0\left(1 - \frac{a^2}{2}\frac{f e^{-f/2}}{f-2} + O\left(a^4\right) + ...\right). \end{aligned} \tag{14}$$

A number of interesting and relevant features emerge from these solutions: first, only even powers of a appear in the expansions. This is a consequence of the symmetry built in to the system: when $\phi_L = \phi_R$ and $f_\mu = 1$, electron particle transport from left to right is equal to hole particle transport from right to left. In both the exponential and step-like cases above, holes encounter an expansion in the EDOS along their transport direction, which increases the hole current. Conversely, electrons encounter a constriction, which decreases the electron current. To linear order (and all odd orders) in the expasion/contraction parameter a, these effects cancel each other so that the total charge current only appears with even powers of a. If the electron/hole symmetry is broken, or the symmetry of the EDOS is reduced (by shifting the step away from the center of the device), then odd powers of a are present (with prefactors whose magnitude reflects the degree of symmetry breaking).

The other relevant feature of Eqs. (12) and (14) is the small magnitude of the a^2 prefactor. Noting again that f is generally larger than 1 for the applied voltages of interest to solar cells, it's clear by inspection that the prefactors are much smaller than 1. This indicates that the effect on transport of a spatial variation of the EDOS is quite weak.

The intuitive picture that emerges from this analysis is that electrons and holes can very easily "squeeze" through regions of reduced density. A natural question concerns the way in which transport is ultimately "pinched off" by letting the density vanish at a point in space. This is shown in Fig. (2), which shows the current in the step-like structure as $a \to 2$. The way in which the current vanishes is very steep; it is only at very small values of EDOS at the cathode that the current drops appreciably (in this limit, the approximation $a \ll 1$ used in deriving Eq. (14) is not satisfied, hence the discrepancy between exact solution and Eq. (14)). However, for very small values of HOMO and LUMO density in real systems, the model presented here is likely not appropriate. This point is discussed more fully in the conclusion.

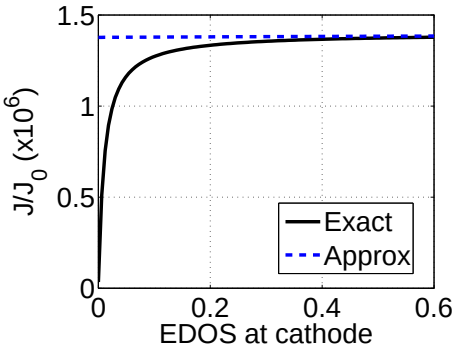

FIG. 2: Extinction of current when EDOS goes to zero. This is for the step-like change in EDOS, for parameters $G = 10^{-9}$, $V_{\rm A} = 0.7$. Both approximate and exact values are shown (where the approximate expression is given by Eq. (14)). It is seen that the current decreases substantially only when the EDOS is nearly zero (or when a is nearly 2).

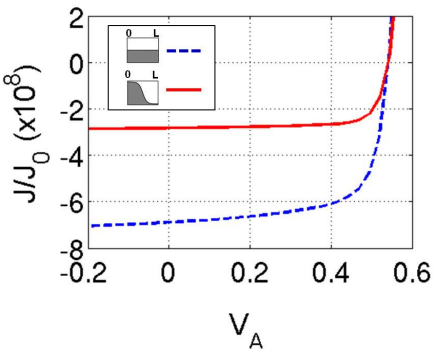

FIG. 3: Current density-Voltage relation for two spatial profiles of D-A EDOS profiles. Blue dotted line is for uniform EDOS profile, red line is for S-shaped EDOS profile, given by Eq. (18)

IV. NUMERICAL STUDIES

I next consider the effect of spatially varying EDOS when the Poisson equation for the electric potential and bimolecular recombination are included. Recall that the dependence of the generation and recombination on EDOS of electron N and hole P is described generically as:

$$\tilde{P} \times G_0 \times g\left(N,P\right) - \left(1-\tilde{P}\right) \times R \times r\left(N,P\right) \ . \quad (15)$$

I make the following ansatz for g (the main conclusion can be formulated in a way that's independent of this specific choice for g):

$$g\left(N,P\right) = P^2 N \ . \quad (16)$$

This is motivated by the observation that the D-A interfacial area requires both P and N, hence g has a factor of each; an extra factor of P is added since the exciton is initially generated in the donor. r is taken simply to be 1, since R already has N and P dependence built in through n and p. Adding a factor of P to the recombination (so that the N,P-dependence of both generation and recombination is the same) has only a weak effect on the results.

A range of composition profiles has been explored for the numeric evaluation of device performance, and I present two representative examples here:

$$N_1(x) = 1 - P_1(x) \ = \ \frac{a}{(e^a-1)} e^{ax/L} \ , \quad (17)$$

$$N_2(x) = 1 - P_2(x) \ = \ \frac{1}{2}\left(1 + (1-2a)\tanh\left(\frac{x-x_0}{\lambda}\right)\right) . \quad (18)$$

Fig. (3) shows the $J-V$ curves for the (N_2,P_2) case (Eq. (18)) for the uniform profile ($a = 1/2$), and a sharp S-shaped profile ($a = 0.95$). Note that the effect of the EDOS profile on the short circuit current $J_{\rm sc}$ is substantial, while the effect on open circuit voltage $V_{\rm oc}$ is small.

The previous analysis can explain the relative insensitivity of $V_{\rm oc}$ to a nontrivial EDOS profile: the effect of a varying EDOS profile on transport is weak, so that the injected current required to offset the photogenerated current (and the corresponding required voltage - $V_{\rm oc}$) is only weakly sensitive to changes in EDOS [16].

The change in $J_{\rm sc}$ can be understood as a direct consequence of the model construction. $J_{\rm sc}$ is the current collected in the absence of an applied voltage, that is, in the absence of charge injected from the contacts. As such it is simply equal to the total charge generation rate in the device: $J_{\rm sc} = \int dx \left(\text{Generation}(x) - \text{Recombination}(x)\right)$. As described above, this is directly parameterized as:

$$J_{\rm sc} \ = \ \int dx \left(\tilde{P} \times G_0 \times g\left[N(x),P(x)\right] - (1-\tilde{P}) \times R \times r\left[N(x),P(x)\right]\right) . \quad (19)$$

In analyzing the effect of $N(x), P(x)$ on $J_{\rm sc}$, it is instructive to separate the N,P dependence of the generation from the above integral. This leaves a quantity δU which depends only on the geometry of the D-A EDOS profile:

$$\delta U \ = \ \int dx \ g\left[N(x),P(x)\right] \quad (20)$$

$$= \ \int dx \ N(x) P^2(x). \quad (21)$$

Strictly speaking the integral in Eq. (19) does not factorize in a manner that leads lead directly to a δU term. However, as I show in the following, δU is a good predictor of the effect of the geometry of the EDOS on the device performance.

For each EDOS profile, I also vary other system parameters. The three different parameterizations are shown in Fig. (4). In system 1, HOMO/LUMO levels are

aligned with cathode/anode Fermi levels ($\phi_L = \phi_R = 0$), and electron and hole mobility are equal. For system 2, $\phi_L = \phi_R = 0$, but electron and hole mobilities are not equal ($\mu_e = 10\mu_h$). In system 3, the HOMO/LUMO are offset from cathode/anode by 0.2 eV ($\phi_L = \phi_R = 0.2$ eV), and electron/hole mobilities are equal.

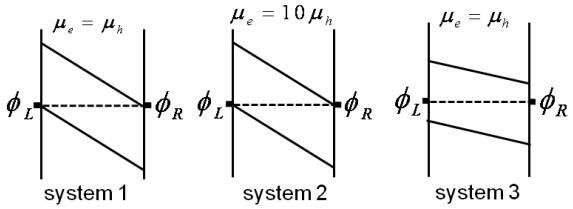

FIG. 4: Cartoon of the three system parameterizations: system 1: $\phi_L = \phi_R = 0,\ \mu_h = \mu_e$, system 2: $\phi_L = \phi_R = 0,\ \mu_h = 10\mu_e$, system 3: $\phi_L = \phi_R = 0.2$ eV, $\mu_h = \mu_e$

Fig. (5a) and (5b) shows δU as the profile parameter a is varied, for various EDOS configurations given by Eqs. (17) and (18), respectively. This is shown for the three system parameterizations. The overall device efficiency η tracks δU very closely for all of these cases (the efficiency is proportional to the maximum absolute value of (JV) in the 4th quadrant of the $J - V$ plane). For this reason I conclude that the primary effect of a spatially varying EDOS on device performance is to change the total carrier generation rate and ensuing $J_{\rm sc}$. δU in Fig. (5) is calculated using Eq. (21), however the conclusion is valid for any choice of g I've tried. Hence the effect of a nonuniform blend on performance can be approximately specified in the generic form given by Eq. (20).

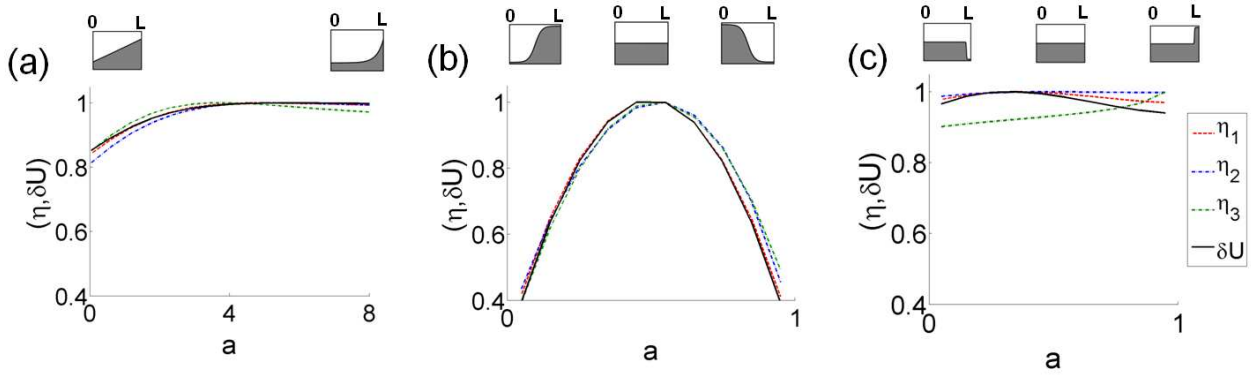

FIG. 5: The efficiency η and geometrical factor δU (normalized by their maximum value) versus geometrical parameter a for (a) exponentially varying profile ($N_1(x)$ of Eq. (17)) (b) S-shaped profile $N_2(x)$ of Eq. (18), with $x_0 = L/2$, $\lambda = L/8$), (c) "skin" layer geometry. Representations of the spatial variation of EDOS as a function of a are shown above the figure. The gray and white regions represent $N(x)$ and $P(x)$, respectively. The efficiency closely follows the geometrical factor δU for most cases. For each geometry I use the three system parameterizations described in Fig. (4) (the subscript of η specifies the system parameterization).

Next I turn to the experimentally motivated geometry of a skin layer of D near the cathode. It's parameterized as:

$$N(x) = 1 - P(x) = \frac{2+a}{4} + \frac{2-a}{4}\tanh\left(\frac{x - x_0}{\lambda}\right), \tag{22}$$

with $\lambda = 0.0075\ L$, $x_0 = 0.05\ L$. Fig. (5c) shows how the efficiency evolves as the skin layer goes from mostly D-like (small a), to an even D-A mix, to mostly A-like (large a) (the experimentally realistic case is smaller a). The change in efficiency is a rather small effect for all three cases (a maximum of 10 % change). Also shown is the geometrical factor δU (solid line). The efficiency of system 1 conforms most closely to the geometrical factor profile dependence. Inspection of the $J - V$ curves for the three systems reveals subtle differences in the fill-factor between the three; there is no simple or obvious source for the difference in behavior between the three system parameterizations. The difference in behavior between the three systems is more conspicuous for the skin layer geometry because the effect of a nonuniform blend is smaller for the skin layer, so that the overall performance is more sensitive to other system parameters. (When the blend profile leads to larger effects, for example that shown in Fig. (5b), there is a similar de-

pendence of device performance on profile for all system parameterizations.) Nevertheless, the important conclusion common to all three system parameterizations of the skin layer geometry is that the effect of the skin layer is small. Its smallness can be understood in terms of the analysis of the previous sections. The analytic work points to the fact that the effect of blend non-uniformity on charge transport is generically small (except in extreme cases). The numerical work of the previous test cases indicates that the effect of blend non-uniformity can be understood in terms of its effect on charge generation and resulting $J_{\rm sc}$ - and that this effect is essentially geometrical (see Eq. (20)). Since a skin layer is by definition geometrically small, its effect is similarly small.

V. CONCLUSION

In this work I presented a simple model for the effect of nonuniform blend profiles on OPV device performance. The main effect of a nonuniform D-A blend is on the the charge generation and resulting short-circuit current: in regions where the blend is primarily of one type at the expense of the other, there is less charge generation due to a reduced D-A interfacial area. The details of how charge generation depends on local blend mix are complicated, and involve almost all aspects of OPV device operation (e.g optics [19], exciton diffusion [7], etc.). The influence of a nonuniform blend on electron and hole transport is a weaker effect.

It's important to appreciate the simplicity of the model presented here relative to the complexity of real OPV devices. Two simplifications of the model are: its treatment of the metal-organic interface, and its restriction to 1 spatial dimension. I make no attempt to capture the effect of a skin layer geometry on the metal-organic contact. The physics at this interface is included most simply as a finite recombination velocity [22] (which can also depend on temperature and field [23]). A hallmark of less effective charge collection/injection at this interface is S-shaped $J-V$ curves [24]. This feature is correlated to metal contact deposition techniques [24], and is not ubiquitously observed in devices. I therefore conclude that the details of the metal-organic contact is not directly tied to the phase segregation in the organic blend.

A more severe approximation of this model is its restriction to 1-d. When the EDOS is small, the charge and current density is also small. However, experiments reveal localized hot-spots of conducting paths [8]. A 1-d model necessarily averages these localized hot-spots or large current density over the entire cross-sectional area, leading to a diffuse current. As the overall area of hot-spots decreases, the charge and current density they must accommodate increases, and current may become space-charge limited. A 1-d model is unable to capture the physics described in this scenario. However for less extreme cases, the treatment described here offers the simplest account for a spatially varying blend structure.

I acknowledge very useful discussions with Behrang Hamadani and Lee Richter.

[1] C. W. Tang. Two-layer organic photovoltaic cell. Appl. Phys. Lett. **48**, 183 (1986).

[2] G. Yu, J. Gao, J. C. Hummelen, F. Wudl, and A. J. Heeger, Science **270**, 1789 (1995).

[3] Jiangeng Xue, Barry P. Rand, Soichi Uchida, and Stephen R. Forrest. J. Appl. Phys., **9**, 124903 (2005).

[4] J. Peet, J. Y. Kim, N. E. Coates, W. L. Ma, D. Moses, A. J. Heeger, and G. C. Bazan. Nat. Mater. **6** 497 (2007).

[5] S. H. Park, A. Roy, S. Beaupre, S. Cho, N. Coates, J. S. Moon, D. Moses, M. Leclerc, K. Lee, and A. J. Heeger. Nat. Photon. **3** 297 (2009).

[6] D. Cheyns, K. Vasseur, C. Rolin, J. Genoe, J. Poortmans, and P. Heremans. Nanotechn. **19**, 424016 (2008).

[7] 1 R. Pandey and R.J. Holmes, Adv. Mater. **22**, 5301-5305 (2010).

[8] B.H. Hamadani, S. Jung, P. M. Haney, L. J. Richter, and N. B. Zhitenev, N.B. Nano letters **10**, 16111617 (2010).

[9] D.S. Germack, C.K. Chan, R.J. Kline, D.A. Fischer, D.J. Gundlach, M.F. Toney, L.J. Richter, and D.M. DeLongchamp, Macromolecules **43**, 3828 (2010).

[10] Z. Xu, L. Chen, G. Yang, C. Huang, J. Hou, Y. Wu, G. Li, C. Hsu, and Y. Yang, Advanced Functional Materials, **19**, 1227 (2009).

[11] P. Schilinsky, C. Waldauf, and C.J. Brabec, App. Phys. Lett. **81**, 3885 (2002).

[12] S. J. Fonash, *Solar Cell Device Physics* (Academic Press, Inc., London, 1981).

[13] B. V. Andersson, A. Herland, S. Masich, and Olle Inganas. Nano Lett. **9** 853, (2009).

[14] L. J. A. Koster, E. C. P. Smits, V. D. Mihailetchi, and P. W. M. Blom, Phys. Rev. B **72**, 085205 (2005).

[15] The most relevant region of the current-voltage relation is in the 4th quadrant. In this region, $V_{\rm A} < E_g$; the different between E_g and $qV_{\rm A}$ is scaled by $1/k_{\rm B}T = 40\,({\rm eV})^{-1}$, so that f is generally much larger than 1.

[16] The change in $J_{\rm sc}$ induced by a spatially varying EDOS has some effect on $V_{\rm oc}$ as well, but this is also a small effect, as $V_{\rm oc}$ generically varies only logarithmically with $J_{\rm sc}$.

[17] H. K. Gummel, IEEE Transactions on Electron Devices, **11**, 455 (1964).

[18] R. Sokel and R. C. Hughes, J. Appl. Phys, **53**, 7414 (1982).

[19] Adam J. Moulé, Jörg B. Bonekamp, and Klaus Meerholz, J. Appl. Phys. **100**, 094503 (2006).

[20] L. Braun, J. Chem. Phys. **80**, 4157 (1984).

[21] L. Onsager, J. Chem. Phys. **2**, 599 (1934).

[22] J.C. Scott and G.G. Malliaras, Chem. Phys. Lett. **299**, 115-119 (1999).

[23] S. Lacic and O. Ingana?s, J. Appl. Phys. **97**, 124901 (2005).

[24] A. Wagenpfahl, D. Rauh, M. Binder, C. Deibel, and V.

Dyakonov, Phys. Rev. B **82**, 115306 (2010).